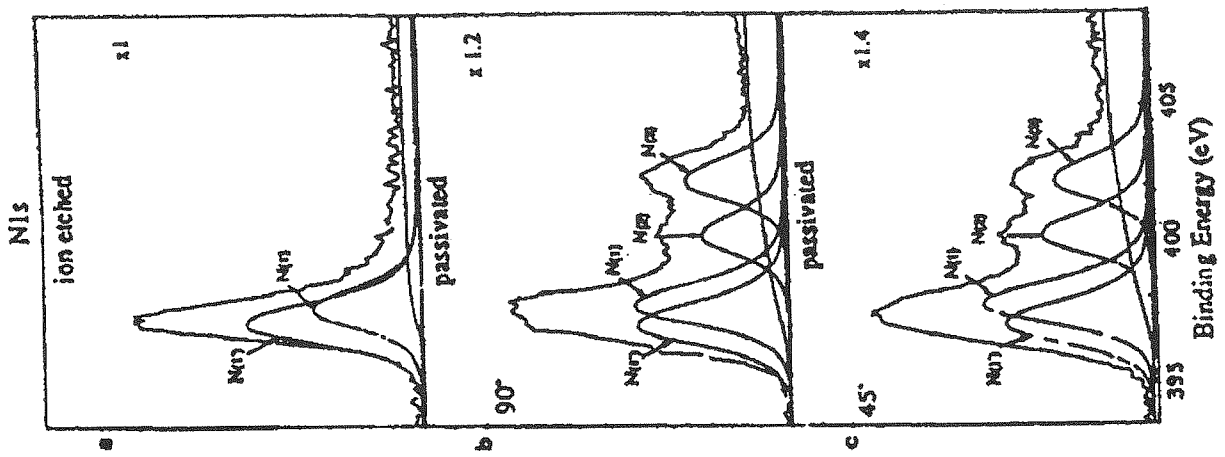

Figure (10) XPS spectra of N1s(N-implanted sample) (a) before passivation, (b) after passivation take of angle 90 (c) after passivation take of angle 45. (0.5M H_2SO_4 +04M NaCl, 650m V/SHE, 30min).

References

[1] HG.French, SD. Cook and RJ. Haddad. J. Biomed Mater Res. 18° (1984) 817.

[2] M.Finnegan. Crit Rev Biocompat 5 (1989)1.

[3] G.Dearnaley, PD. Goode, FJ. Minter and AT. Peacock. J. Vac Sci. Technol.3 (1985) 2684.

[4] TW.Barbee, BE. Jacobson and DL. Keith. Thin Solid Films.63 (1979) 143.

[5] A.Billard, M. Foos, C. Frantz and M. Gantois. Proceeding of 8th Int. Conf. on Thin Films 8-12 June 1990, San Diego, USA.

[6] D.Sundararaman, P.Kuppusami and VS. Raghunathan. Surf Technol. 18 (1983) 341.

[7] ZL. Zhang and T.Bell. Surf Eng. 1 (1985) 131.

[8] SM. Ficher, A. Viaje, GD. Mills and TJ. Slaga. In: Williams JR (Ed). Methods in cell Biology. Vol21 A. New York: Academic Press, (1980) 207.

[9] PJ. Marie, A. Lomry, A. Sabbagh and M. Basle. In Vitro Cell Dev Biol. 25(1989) 373.

[10] OA. Bessey, OH. Lowyand MJ. Brock. J Biol Chem. 164 (1946)321.

[11] C.A. Straede, Wear 130 (1989)113.

[12] G.D. Lempert, Surf. Coat. Technol. 34 (1988) 185.

[13] F.G. Yost, S. T. Picraux, D. M. Folstaedt, L. E. Pope and J. A. Knapp, Thin Solid Films 107 (1983) 287.

[14] S.Fayeulle, D. Treheux and C. Esnouf, Mater. Sci. Eng. 25 (1986) 288.

[15] M.Iawaki, T. Fujihana and K. Okitaka, Mater. Sci. Eng. 69 (1985)211.

[16] C. Chabrol, R. Leveque. Mem. Et. Sci. Rev. Met. 85. No1 (1988) 43.

[17] I.Olefjord, Mat. Sci. Eng., 42(1980) 161.

[18] A. Sadough, R. Chikhi and P. Marcus, Preoceedings of UK CORROSION and EUROCORR 94. Vol. 1 Bournemouth, 31 Oct-3 Nov (1994) 169.

[19] C.Sarrazin, D. desjardins, J. M. Ilive, R. Karray. Mem. Et. Sci. Rev. Met. 88. No11 (1991) 761.

[20] P.Marcus and M. E. Bussell, Appl. Surf. Sci. 59(1992)7.

[21] E. De Vito and P. Marcus Surf. Interface Analysis, 19(1992)403.

[22] E. De Vito and P. Marcus Proceeding of the 12th International Corrosion Congress, Houston Texas, USA, NACE International, Vol 53 (1993) 3898.

[23] A. Sadough Vanini Amirkabir J. Sci. Technol. Vol. 11. No. 42; (2000)47.

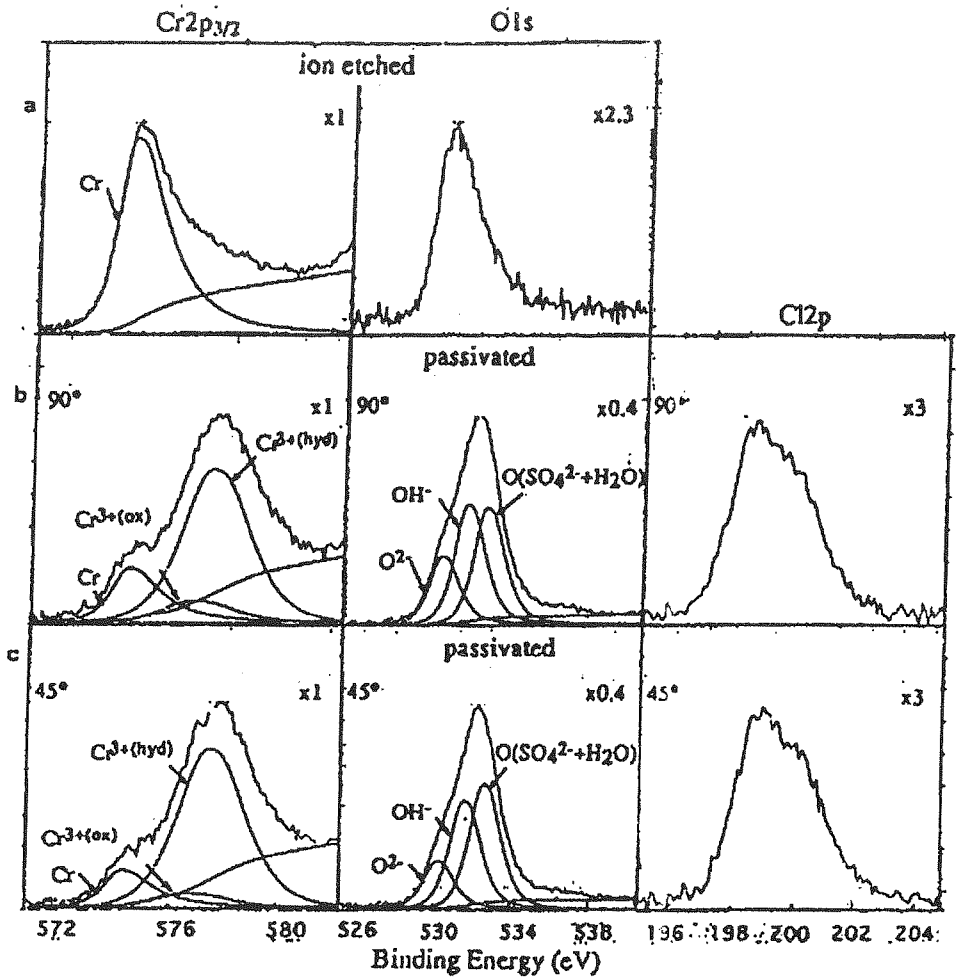

Figure (9) XPS spectra of $Cr2p_{3/2}$, O1s and C12p(Mo-implanted sample)(a) Before passivation, (b) after passivation take of angle 90 (c) after passivation take of angle 45. (0.5M H_2SO_4 +0.4M NaCl, 650mV/SHE, 30min).

Tableau (1) Electrochemical data for the different studied alloys.

Sample	Corrosion potential (mV/SHE)*	Potential at the peak max. (mV/SHE)	Current at the peak max. ($\mu A/cm^2$)**	Current in the passive state ($\mu A/cm^2$) ***
Mo-N-imp R1	-115	68	78	1.5
Mo-N-imp R2	-110	78	50	1.8
Mo-imp	-10	55	48	2
N-imp	-144	48	43	2.3
Unimp	-140	90	100	1

*: potential measured at the maximum of the activation peak.
**: Current density measured at the maximum of the activation peak.
***: Minimum measured current density in the passive state.

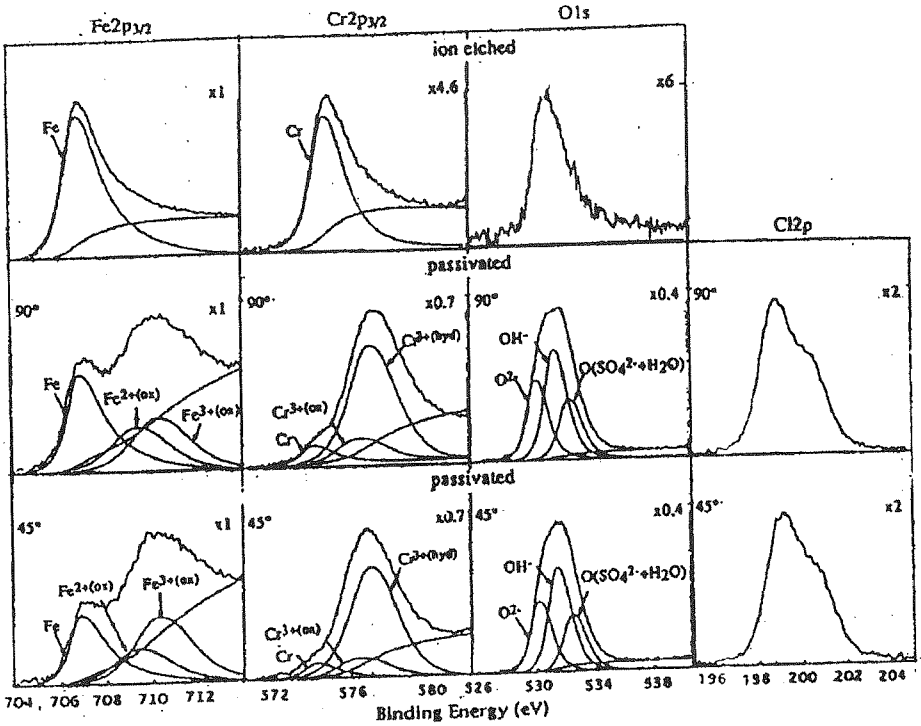

Figure (7)XPS spectra of $Fe2p_{3/2}$, $Cr^2p_{3/2}$, O1s and C12p(co-implanted Mo-N sample), corresponding to the first region R1, in the depth profiles (a) before passivation, (b) after passivation take of angle 90 (c) after passivation take of angle 45. (0.5M H_2SO_4 +0.4M NaCl, 650mV/SHE, 30min).

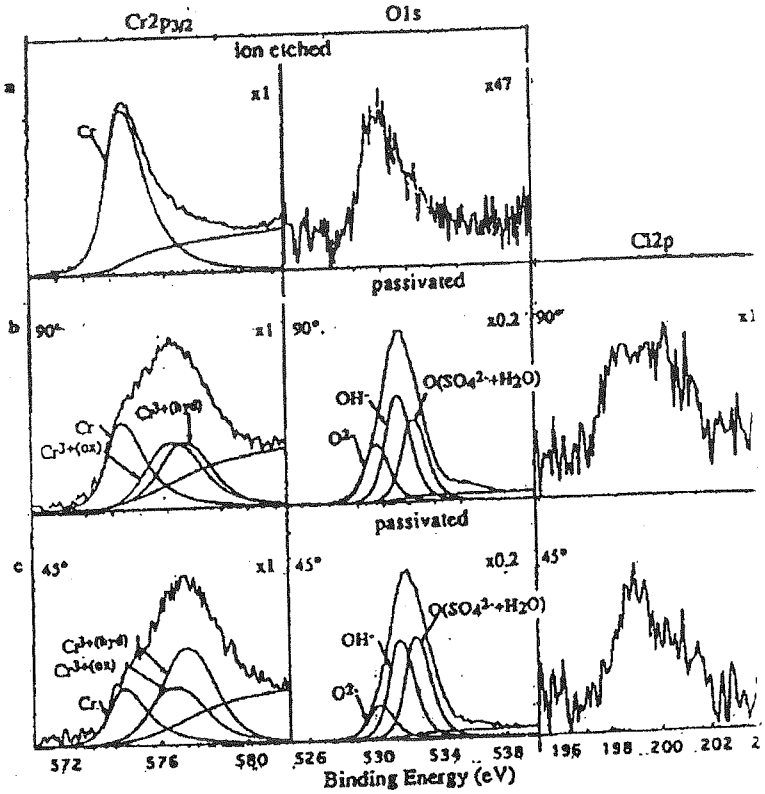

Figure (8) XPS spectra of $Cr2p_{3/2}$, O1s and C12p(co-implanted Mo-N sample), corresponding to the second region R2, in the depth profiles (a) before passivation, (b) after passivation take of angle 90 (c) after passivation take of angle 45. (0.5M H_2SO_4 +0.4M NaCl, 650mV/SHE, 30min).

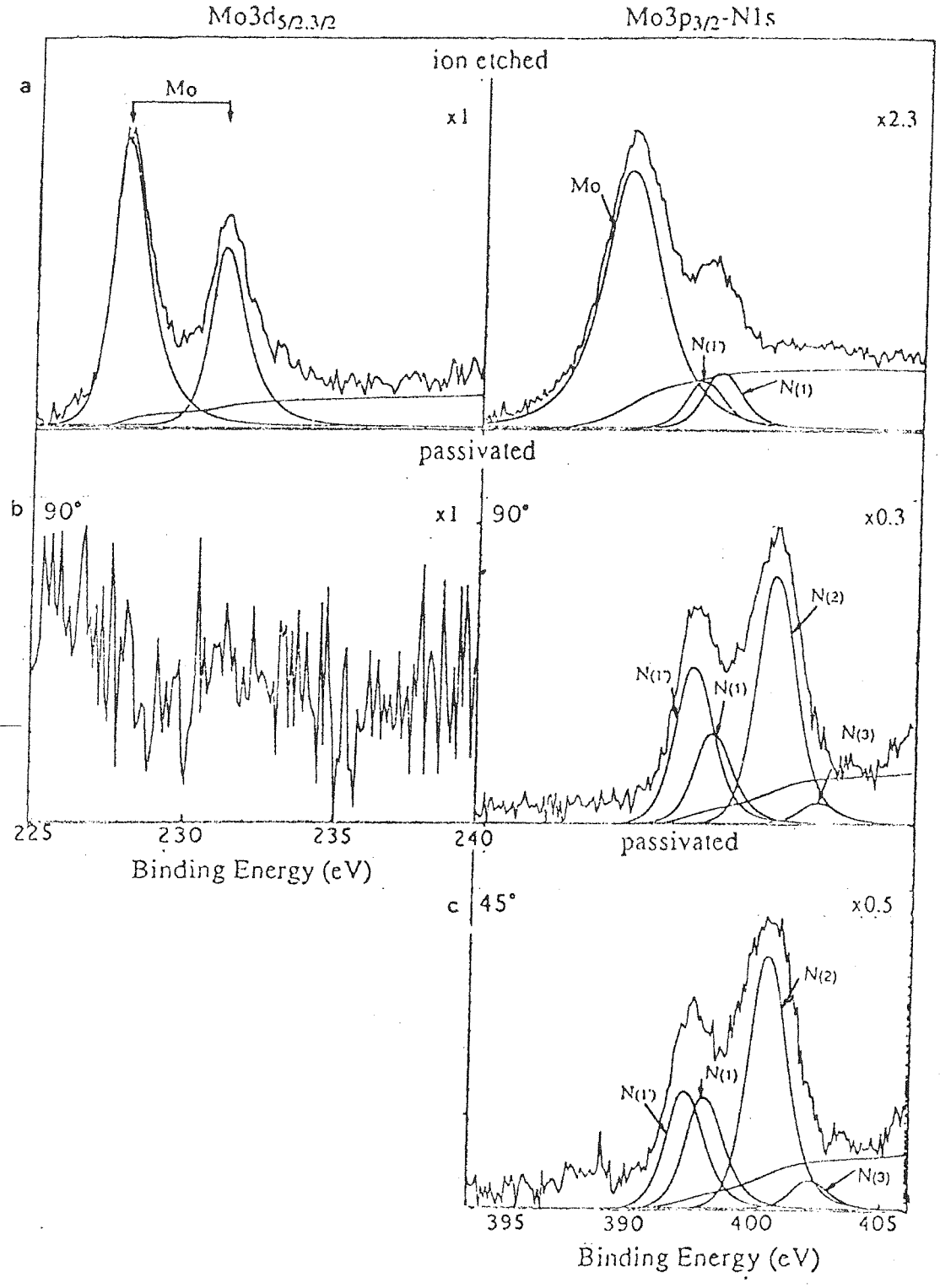

Figure (6) XPS spectra of $Mo3d_{5/2,3/2}$ and $Mo3p_{3/2}$-N1s (co-implanted Mo-N sample), corresponding to the second region R2, in the depth profiles (a) before passivation, (b) after passivation take of angle 90 (c) after passivation take of angle 45. (0.5M H_2SO_4 +0.4M NaCl, 650mV/SHE, 30min).

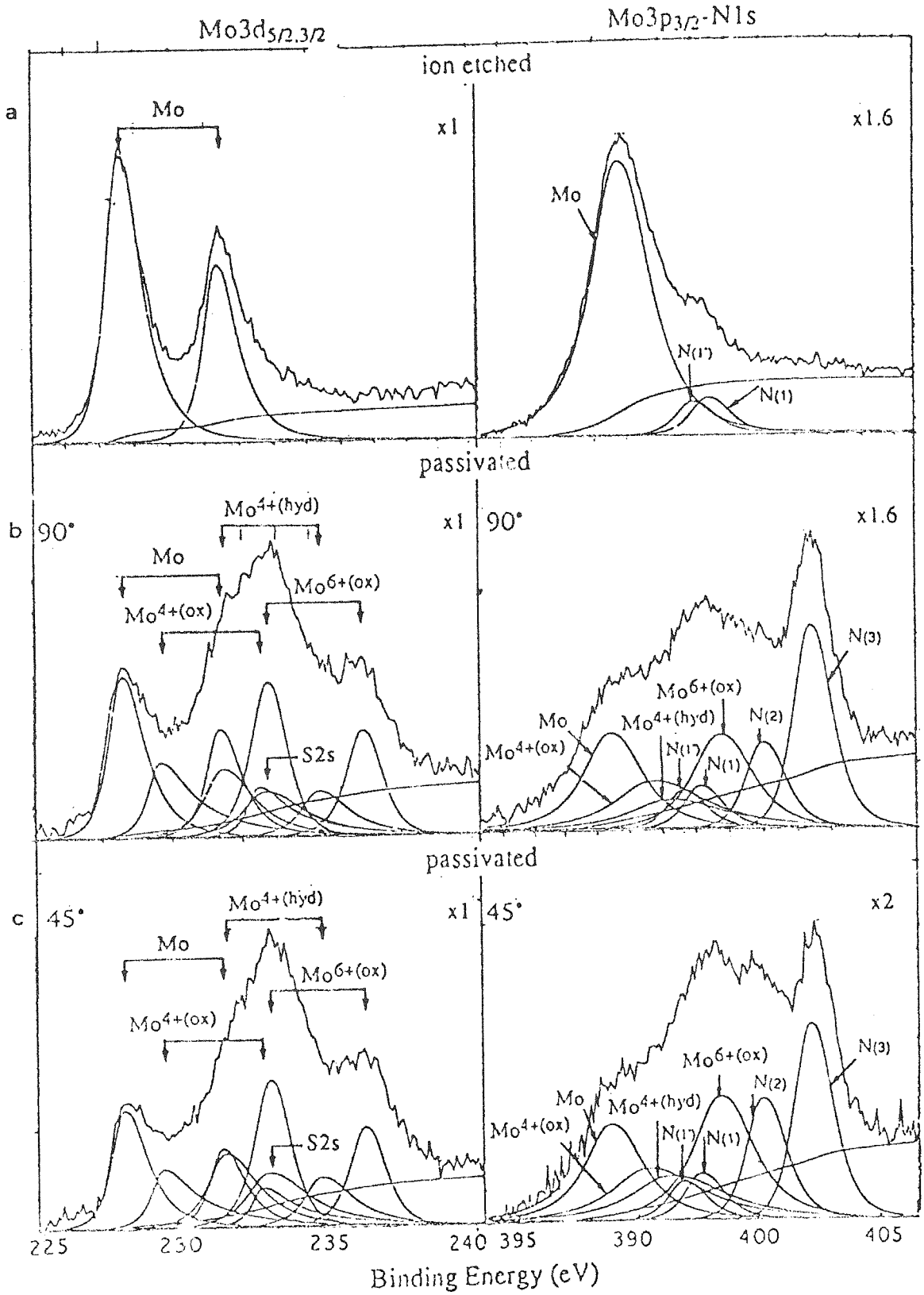

Figure (5)XPS spectra of $Mo3d_{5/2,3/2}$ and $Mo3p_{3/2}$-N1s (co-implanted Mo-N sample), corresponding to the first region R1, in the depth profiles (a) before passivation, (b) after passivation take of angle 90 (c) after passivation take of angle 45. (0.5M H_2SO_4 +0.4M NaCl, 650mV/SHE, 30min).

of unimplanted ones. This behavior can be explained by the increase in the physical or chemical heterogeneity of the sample surface after implantation. In the passive state Cl^- are incorporated in the film. Cl^-, which entered the inner part of the passive film, is the precursors of pit initiation.

Microhardness was strongly improved, especially by nitrogen implantation.

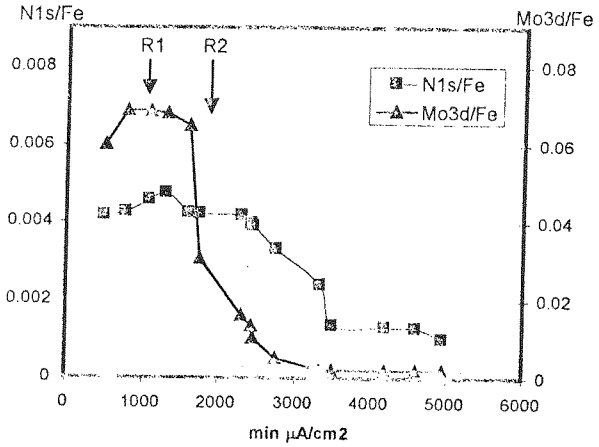

Figure (1) XPS depth profile of Mo and N in the co-implanted austenitic stainless steel.

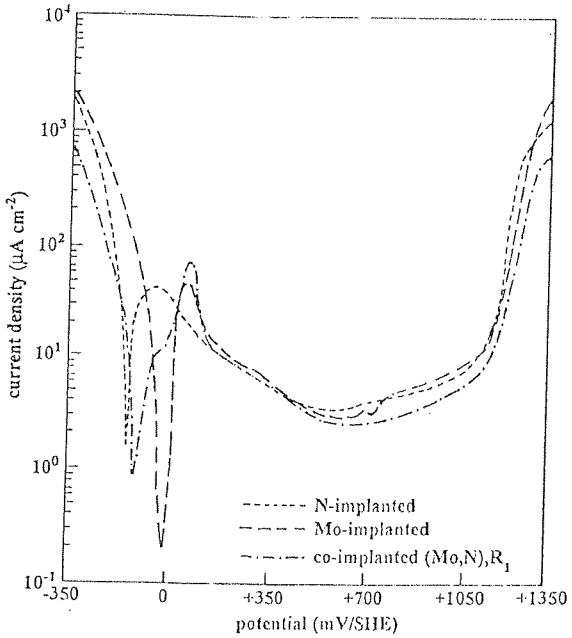

Figure (2) Potentiodynamic curves, comparison between the N-implanted, Mo-implanted and co-implanted (Mo-N) alloys in 0.5M H_2SO_4 +0.4M NaCl

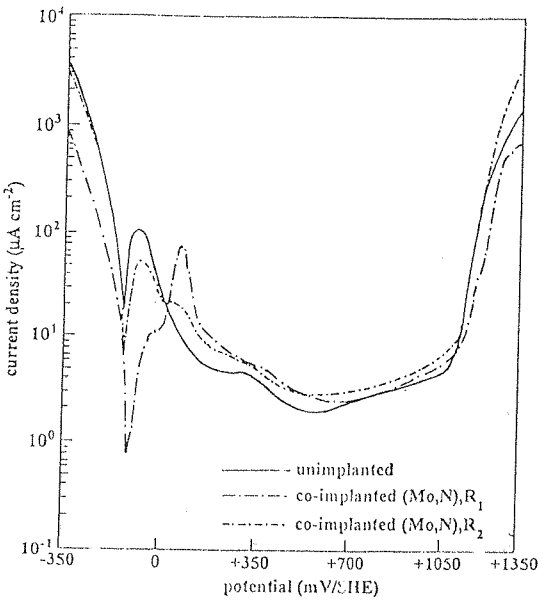

Figure (3) Potentiodynamic curves, comparison between the non - implanted co- implanted (Mo-N) first region in the depth profile R1 and co-implanted (Mo-N) second region in the depth profile R2, in 0.5M H_2SO_4 +0.4M NaCl

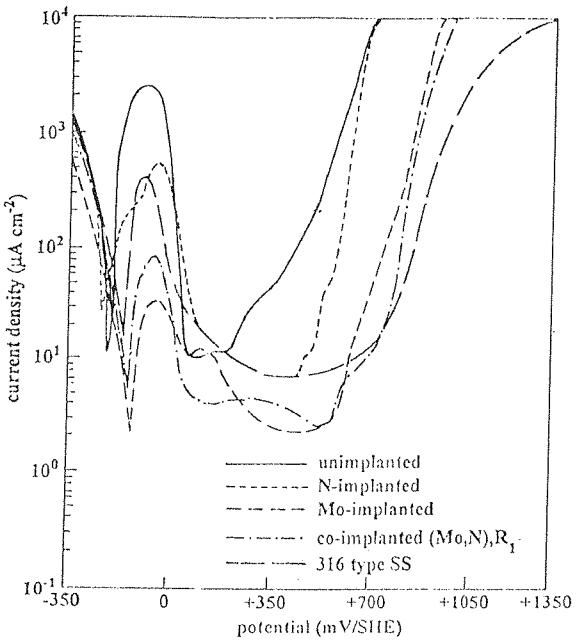

Figure (4)Potentiodynamic curves, in 0.5M H_2SO_4 +0.8M NaCl

chemical heterogeneity of the sample surface after implantation, with the appearance of the numerous defects as a dense dislocation network and formation of the different phases (oxide, nitride, α´-martensite). These defects may supply active sites for pitting.

The XPS spectra for the Cr2p3/2, O1s and C12p obtained for the Mo-implanted alloy with dose of $2x510^{16}$ atome/cm2 are shown in figure 9. The $Mo3d_{5/2, 3/2}$ spectrum recorded after 15min of ion etching and passivation (not shown here) are similar with what observed for the R1 region of Mo-N-Implanted samples, also this result demonstrates that the implanted molybdenum participates in the psassivation of the alloy. The $Cr2p_{3/2}$ region indicates a marked enrichment of this element in the passive film. In this region low intensity of the peak at low binding energy confirm the previous idea that in the passive film of nitrogen implanted alloy Cr bonded to nitrogen.

The XPS spectra for the N1s obtained for the N-implanted alloy with dose of 2×10^{17} at/cm^2 are shown in figure 10.The N1s spectrum recorded after 15 min of ion etching shows a large N1s. These results indicate that nitrogen is enriched at the surface and is incorporated in to the passive film. In the Cr2p3/2 spectrum the peak at low binding energy is similar with what was observed for the R2 region in co-implanted alloy (not shown here). The intensity of this peak is lower for the 45 take of angle. In an attempt to obtain a clear picture of the chemical state of nitrogen in the passive film, the N1s spectrum was fitted by four peaks in figure 10. The peak located at low binding energy N(1´) (397 eV) is attributed to the implanted nitrogen. The intensity of N(1´) is higher for the ion-etched sample. The peak located at medium binding energy N(1) (397. 7eV) is assigned to N1s electrons emitted by Cr-N incorporated in the film. The peak located at higher binding energy N(2) at 400.2eV) may originate from N-H or N-O (19). The forth peak located at an even higher binding energy (N(3) at 402eV), originates from nitrogen which may be under the form of NH^{4+}(8).

The microhardness of Mo-N-implanted SS was 6-7 times higher than that of untreated material. In the surface corresponding to the maximum of nitrogen concentration in the profile the microhardness was between HV 0.3N 11000 MPa and Hv 0.3N 12000MPa. The same levels of microhardess were found for N-implanted SS.

The effect of ion implantation on the biocompatibility of 304 SS was studied, our preliminary cell culture results indicate that ion implanted SS were biocompatible. Nitrogen and molybdenum implantation could be efficient means for improving the physical properties of SS without affecting it biocompatibility.

Concllusion

The effects of the ions implanted molybdenum and nitrogen on the electrochemical behavior of the alloy in 0. 5 M H_2SO_4 +(0. 4M NaCl or 0. 8M NaCl) have been investigated. The surface films have been analyzed by XPS.

The high potential region of passivity is similar for the two concentrations of Mo-N, Mo-implanted, N-implanted and for unimplated alloys in 0.5M H_2SO_4 +0.4M NaCl solution. A slightly higher residual current density observed in small Mo-high N concentration region.

In high concentration of chloride 0.8M NaCl+0.5M H_2SO_4 the pitting potential of implanted alloy is always lower than that of 316 type stainless steel and higher than that

were polarized 30 minutes. The samples were then removed from the cell under the applied potential, rinsed in ultra-pure water, dried in nitrogen and transferred to the spectrometer without exposure to ambient air.

The XPS spectra for the $Mo3d_{5/2,\ 3/2}$ and $Mo3p_{3/2}$-N1s obtained for the co-implanted Mo-N sample before and after passivation corresponding to first and second regions (denoted R1 high Mo-high N and R2 small Mo-high N respectively) in the depth profiles, are shown in the figures 5 and 6. The Mo3d and 3p signals have been resolved into the metallic form (Mo implanted in the alloy) and three oxide states: Mo^{4+ox} (MoO_2 type), Mo^{4+hyd} ($MoO(OH)_2$ type) and Mo^{6+ox} (MoO_3 type). The curve fitting of the Mo spectrum show that Mo is mainly present in the passive film in the form of Mo^{6+ox}. A small amount of Mo^{4+ox} is also detected.

The XPS spectra of Mo3p-N1s were fitted by 7 peaks: 3 Mo states discussed above and 4 N states. Two nitrogen peaks located at low binding energy (397 and 397. 6eV) are associated to N implanted in the alloy and two nitrogen peaks located at higher binding energies (400.2 and 402 eV) may originate from N-H or N-O (9).

High-resolution spectra for the $Fe2p_{3/2}$, $Cr2p_{3/2}$, O1s and C12p corresponding to R1 and R2 regions are shown in figures 7 and 8. No C12p signal was detected from the samples before passivation. Oxidized iron is found in the passive film though in smaller quantities than chromium oxide. The chromium signal $Cr2p_{3/2}$ region was resolved into chromium oxide Cr^{3+ox} (Cr_20_3 type, binding energy: 576. 6 eV) and chromium hydroxide Cr^{3+hyd} ($Cr(OH)_3$ type binding energy 577.2 eV). The results indicate a marked enrichment in Cr^{3+} in the passive film. The oxygen signal clearly reveals the presence of the oxide (O^{2-}) and hydroxide OH^- forms. A third peak is present at higher binding energy corresponding to oxygen in H_2O and SO_4^{2-}. Angle-dependent XPS analyses have been carried out to obtain further information on the in-depth distribution of the different species. As expected, the signals of the oxidized elements are enhanced with respect to those of the metals at low take off angle. In sharp contrast with what was observed for the passive film in 0.5M H_2SO_4 solution (23). The Cr^{3+hyd}/Cr^{3+ox} ratio does not vary in same way. This result is confirmed by the O^{2-} and OH^- contributions in the O1s signal, which are not affected by the take-off angle. This clearly proves that there is no bilayer structure at this condition. The surface film is a single layer containing the various species.

In the R2 Region, the detected chemical states of chromium are similar to the detected in R1 region. In contrast with what was observed for the R1 region, in $Cr2p_{3/2}$ spectrum a broad intense peak at low binding energy is believed to be associated with chromium in the underlying alloy and chromium located in the film and bonded to nitrogen (20). The $Cr.^{3+hyd}/Cr^{3+ox}$ ratio is enhanced in the angular analysis at the take-off angle (45). This reveals the layered structure of the passive film: the chromioum hydroxide is found to be in the outer part of the passive film (enhanced signal at 45) whereas chromium oxide is in the inner part. The O1s signal, which has an OH - component partly related to Cr^{3+hyd} shows the same tendency. The major difference between the surface composition in the R2 and R1 regions is observed in the Mo signal which reveals that in the R2 region the molybdenum does't present in the passive film, but is present before passivation. This behavior can be explained by high dissolution in chloride solution and by the increase in the physical or

1-Electrochemistry of the implanted alloy

Prior to passivation experiments, the implanted alloys were sputtered to obtain the different concentrations of Mo and N indicated by R1 and R2 in the depth profiles. Also the unimplanted, Mo-implanted and N-implanted alloys were examined for comparison. The Mo-implanted and N-implanted alloys were sputtered for 15 minutes. This sputtering procedure yields surfaces , corresponding to, Mo. concentration 7 atomic % for the alloys implanted with Mo. and 10.5 atomic % for the alloy implanted with N. The surfaces were analyzed by XPS prior to sample transfer to the glove box where the electrochemical potential scans (1 mV/s) were carried out from - 350 to 1350 mV/SHE. These i-E plots in deaerated 0.4M NaCl+0.5M H_2SO_4 solution are reported in fig 2 and 3 while the corrosion parameters of the materials are listed in table 1. As the concentration of Mo decreases and the nitrogen increases it is observed that the current in the active region of the polarization curves increases, in agreement with other published data (20, 22). For the high concentration of Mo the activation peak disappears, and the residual current density is higher in the 100-300 mV/SHE potential region, where an oxidation or dissolution process occurs. This may be result from defect concentration introduced during Mo-N implantation. Knowing that the profile of the defects is near to the surface in this case the R2 region in the depth profiles of Mo-N does not superpose to the defect profile. This finding and comparison between residual current density in co-implanted Mo-N R1 and R2 regions support the view that the defect concentration are active sites for oxidation or dissolution. The high potential regions of passivity are similar for all samples. Shift of corrosion potential to more negative values with diminution of Mo concentration and presence of N in high quantity may be due to an increase of the overvoltage for the hydrogen evolution reaction or to enhanced anodic dissolution. These results indicate that the implantation of Mo-N had a beneficial effect on the protective character of the passive film in 0.4M NaCl+0.5M H_2SO_4 solution. Additional tests were conducted in a deaerated 0.8M NaCl+ 0.5M H_2SO_4 solution. Figure 4 shows the anodic polarization curves for co-implanted (Mo-N), Mo-implanted, N-implanted and unimplanted, alloys. The polarization curve for 316-type stainless steel is also included in the figure for comparison. The results show that (i) in the active region the dissolution current densities are in the following order:unimp>N-imp>316SS>co-imp>Mo-imp, (ii) the active/passive transtion potential (maximum in the i-E curve) is shifted to more anodic potentials when the Mo concentration increases. (iii) The current in the passive state decreases with increasing Mo concentration and (iv) the pitting potential, which is observed for all investigated alloys, increases for increasing N and Mo concetration. Note that unimplanted alloy exhibited a small range of passivity up to about 0.2 V/SHE followed by a rapid increase in current density. At the end of the test, the specimen surfaces were examined under a microscope and pits were visble in all investigted alloys.

2-Surface analysis results

For the XPS study of the passive films, the potential was stepped to 650 m V/SHE (which is in the passive region, for all analysis samples) in 0.4M NaCl+0.5M H_2SO_4 for the two take of angle (45,90) and the samples

composition, chemical states and resistance to localized corrosion of passive films on N and Mo implanted austenitic stainless steel in acidic solution without Cl ion have been characterized in previous work (23). In the present work a combined XPS and electrochemical study was performed on 304 type SS implanted with Mo and N and passivated in an acidic aqueous solution containing Cl ions. The effects on pitting potential of the presence of Cl ion in the passivation solution and N and Mo implantation were investigated. The passivated films formed for concentrations of Mo and N were analyzed by XPS, and their compositions were also studied as a function of Mo-N concentration. More directly in this part of work, we seek to understand how the joint effects of Mo and N during passivation in chloride-containing media.

Experimental procedure

Conventional austenitic stainless steel (AISI 304 type) having the following composition (wt%): Cr (17.38), Ni (8.28), Mn (1.43), Si (0.49), Cu(0.15), Mo(0.14), C(0.05), N (0.04), P(0.03) and S(0.0025) and Fe (balance), were used.

The one milimeter thick samples were implanted with Mo and N co-implanted first with Mo and then with N ions (100 Kev, 10^{-5} torr, at room temperature). The implantation conditions described in greater detail elsewhere (23). Sample discs of 10 mm diameter were cut from the implanted steels by spark erosion, ultrasonically cleaned with acetone and rinsed in ethanol and pure water. XPS studies have been performed with a VG ESCALAB Mark II spectrometer using Al Kα X-ray source ($h\nu$=1486.6 eV) and a hemispherical analyzer with a pass energy of 20 eV for the high-resolution spectra. The reference for the reported binding energies are Au4f7/2 at 83.8 eV and Cu2p3/2 at 932.7 eV. Depth profiles were obtained by sputtering the surface with argon ions. A VG AG 21 ion gun mounted in the preparation chamber attached to the spectrometer was used. The sputtering conditions for the preparation of the samples before passivation were 2 kV, pAr = 7×10^{-6} mbar and a current density of 100 μA/cm^2. The sample was introduced into the preparation chamber of the XPS spectrometer where it was ion etched and then transferred in a transfer vessel under pure nitrogen into a glove box where the electrochemical experiments were carried out. The electrochemical cell was composed of a saturated sulfate reference electrode, a platinum counter electrode and a working electrode. A PAR 273 potentiostat interfaced with a computer was used. The electrolyte was a 0.5 M H_2SO_4 + (0.4M NaCI or 0.8M NaCI) solution prepared from ultra-pure water, pure sulfuric acid and pure sodium chloride. After passivation, the samples were rinsed in ultra pure water, dried in N_2 ambient and then transferred back to the spectrometer. XPS analysis was then carried out. Microhardness measurements were made using a Vickers indenter, HV 0.3 N.

Results and Discussion

The Nls/Fe2p3/2 and Mo3d/Fe2p3/2 ratios obtained from the XPS depth profile analysis performed on co-implanted SS are shown in Fig. 1 as a function of sputtering time. Simulations of the concentration profiles for the implantation of Mo and N have been performed in previous works (20-22). The maximum in the profile occurs at a depth below the surface of 150Å for Mo and 580Å for N.

Surface modification by ion implantation of 304 stainless steel, orthopedic implants. Part 1.

A.Sadough-Vanini
Associate Professor
Mechanical Engineering Department,
Amirkabir University of Technology

Abstract

In order to improve the wear and corrosion resistance as well as the hardness of 304 stainless steel (SS) for mechanical use, surface treatment derived from those applied in mechanical engineering industries were investigated. Surface characterization according to the different ion implantation showed that corrosion and wear resistances were strongly improved. In the same way, microhardness was significantly increased after ion implantation.

Keywords

ion implantation - corrosion- passivation- electrochemistry-hardness.

Introduction

AISI 304 stainless steel (SS) is widely used in orthopedic implantology although medical complication can result from its mechanical failure and inadequate tribological properties. The chemical conditions within the human body results in corrosive environment for metals, mainly due to the presence of chlorine ions at concentration of (0.11N) in interstitial fluids. Metals in contact with human fluids, from orthopedic implant to body piercing jewelry, must exhibit a high degree of corrosion resistance not only because of the deterioration of the mechanical properties but also the possible physiological effects of harmful or cytotoxic corrosion-products that may be released into the body. Orthodontic bands, brackets, and wires are mainly made of austenitic stainless steel containing approxiately 18%Cr and 8%Ni. Nickel-titanium alloys are also used as orthodontic arch wires and present another source of patient exposure to metals corrosion products. Since the temperature conditions and the presence of the ions, microbes and enzymes in the oral environment is particularly suited for the biodegradation of metals some level of patient exposure to corrosion products of these alloys could be assumed, if not assured. Iatrogenic exposures to Ni,Cr, and Ti can also occur from joint prostheses, dental implants, orthopedic plates and screws, surgical clips and steel sutures, pacemaker leads, prosthetic, heart valves, dental alloys, and orthodontic appliances (1-10).

The efficincy of N and Mo surface treatment to improve the resistance of stainless steels to wear, friction and corrosion have been demonstrated (11-16). Alloyed molybdenum addition is known to improve resistance to localized corrosion in chloride solution. As regards electrochemical behavior and XPS analysis of nitrogen and molybdenum containing (17, 18), nitrogen implanted (19,20) and molybdenum implanted (21,22) austenitic stainless steel, the results are often conflicting. Chemical